Enzyme Optimization and Process Development for a Scalable Synthesis of (R)-2-Methoxymandelic Acid

Mark E. Scott, Xiaotian Wang, Luke D. Humphreys,* Michael J. Geier, Balamurali Kannan, Johann Chan, Gareth Brown, Daniel F. A. R. Dourado, Darren Gray, Stefan Mix, and Aliaksei Pukin

Cite This: https://doi.org/10.1021/acs.oprd.1c00250

Read Online

ACCESS | 📊 Metrics & More | 📖 Article Recommendations | 🆂🅸 Supporting Information

ABSTRACT: The rational protein engineering of wild type BCJ2315 nitrilase and its use in the development of a one-pot, enantioselective, dynamic kinetic resolution for (R)-2-methoxymandelic acid is reported. Through a combination of molecular docking and B-factor analyses, a focused library of mutants was identified and screened to improve nitrilase selectivity, activity, and stability. Initial optimization revealed that the addition of sodium bisulfite prevented enzyme deactivation by the aldehyde starting material, removing the need to isolate the cyanohydrin and allowing for development of a one-pot process for mutant screening. Further optimization of the process with the preferred mutants revealed subtle interactions between temperature, pH, substrate loading, and enzyme source which ultimately led to development of a suitable lyophilized whole cell process for scale-up, affording (R)-2-methoxymandelic acid in 97% ee and 70% isolated yield on multigram scale.

KEYWORDS: nitrilase, mandelic acid, enantioselective, biocatalysis, dynamic kinetic resolution, protein engineering

INTRODUCTION

In the past two decades the application of biocatalysis for the preparation of pharmaceuticals, their intermediates, and commodity chemicals has undergone significant growth and development.[1] Biocatalysts have been more widely adopted by industry due to their selectivity and ability to catalyze a broad range of chemical transformations under mild reaction conditions in green solvents (e.g., water). In addition, biocatalysts can be readily engineered to optimize properties such as stability, activity, and selectivity which allows for the design of robust and scalable processes.

Biocatalysts have been broadly categorized using enzyme commission (EC) numbers.[2] The nitrilase superfamily are hydrolase enzymes (EC3) that catalyze the hydrolysis of nitriles, acid amides, secondary amides, ureas, and carbamates via their catalytic cysteine, glutamate, and lysine triad.[3,4] While each of these nitrilase-mediated synthetic transformations are useful, arguably the most appealing from a process chemistry perspective is nitrile hydrolysis given the ease of introducing nitrile functionalities within synthetic building blocks as a masked carboxylic acid surrogate.

Recently, as part of our process chemistry efforts for a clinical compound, we sought to develop an enantioselective route to the process intermediate (R)-2-methoxymandelic acid. Based upon our initial survey of the literature we were immediately intrigued at the possibility of designing an enantioselective one-pot enzymatic nitrilase approach toward (R)-2-methoxymandelic acid, based on prior successful reports for the parent mandelic acid compound.[5,6] Our initial approach was to leverage a dynamic kinetic resolution (DKR) whereby racemic cyanohydrin **2** is selectively hydrolyzed to the requisite (R)-2-methoxymandelic acid **3** (Scheme 1). Based on related literature precedent for ortho substituted mandelic acid

derivatives,[7] we anticipated several challenges with this approach: avoiding enzyme deactivation from cyanide or aldehyde while achieving high enantioselectivity and identifying a process friendly isolation, including a product crystallization which avoided a concentration to dryness. To this end, this manuscript highlights our approach to addressing these challenges via the concurrent development of a one-pot process and enzyme engineering to address the anticipated enantioselectivity and process robustness challenges, followed by our subsequent downstream process optimization isolation development.

RESULTS AND DISCUSSION

Our initial approach was two-pronged, whereby we concurrently developed suitable conditions for initial nitrilase screening, coupled with a rational *in silico* design of a 96 mutant library that focused on improved enantioselectivity and enzyme stability over the wild-type. Further process refinement was planned to enable robust evaluation of more promising mutants from the first round of enzyme engineering on scale. In turn, this would facilitate a second round of mutants via combination of the best performing mutants from round one.

Initial process development was performed using a previously reported novel nitrilase BCJ2315 isolated from *Burkholderia cenocepacia* J2315.[6] This nitrilase was selected

A

Scheme 1. Proposed One-Pot DKR Route to (*R*)-2-Methoxymandelic Acid (3)
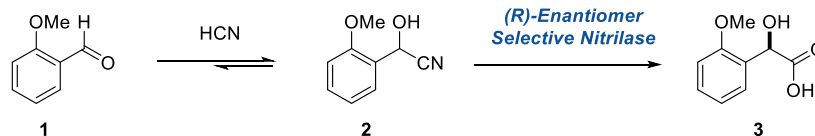
Table 1. Effect of Organic Cosolvents on BCJ2315 Lyophilized Whole Cell Activity[a]

Entry	Solvent (10% v/v)	Substrate concentration (g/L 2)	Enzyme Loading (%, w/w)	Conversion at 3.5 h (%)[b]	Conversion at 16 h (%)[b]	% ee
1	Methanol	10	10	0	0	–
2	Ethanol	10	10	0	0	–
3	Isopropanol	10	10	0	0	–
4	DMSO	10	10	48	67	92
5	MTBE	10	10	5	62	75
6	Toluene	10	10	3	27	85
7	Ethyl acetate	10	10	60	85	90

[a]To 0.1 mL of a solution of **2** in organic solvent was added BCJ2315 (freeze-dried cells) in 0.9 mL of phosphate buffer (100 mM, pH 7.4) followed by shaking at 30 °C. [b]Determined using HPLC at 283 nm. Conversion was determined by [% AN **3** + % AN **ent-3**]/[% AN **1** + % AN **2** + % AN **3** + % AN **ent-3**].

based on prior engineering success to enable the synthesis of (*R*)-2-chloromandelic acid along with a variety of related substituted mandelic acid analogues.[7] We began initial screening studies using isolated cyanohydrin **2** and BCJ2315 wild-type nitrilase from soluble expression in *E. coli* and isolated as a lyophilized cell-free extract (CFE), since this preparation was favored from a process perspective due to its purity and anticipated minimal downstream isolation/workup complications. However, trial reactions using 10% by weight CFE at pH 7.4 with 25% methanol gave only ca. 1% AN of **3** after 63.5 h. Screening was then performed with the CFE to further evaluate cosolvent impact on reaction conversion using 10, 20, 30% (v/v) of methanol or ethanol, or 10% (v/v) of toluene via overnight shaking with 10% by weight enzyme loading relative to **2**. None of the reaction mixtures with alcohol cosolvents contained the product after 16 h of shaking at 30 or 37 °C. On the contrary, reactions that were conducted under biphasic conditions with toluene as a cosolvent afforded minor formation of **3** in all conditions evaluated. From these initial studies the best conditions led to 16% product formation by HPLC using 10% (v/v) in toluene (10 g/L BCJ2315 CFE, 100 g/L of **2**, 100 mM potassium phosphate (pH 7.4), shaken for 16 h at 30 °C).

Based on our initial limited success using lyophilized BCJ2315 CFE enzyme, we re-evaluated the enzyme preparation used for our studies. Previous reports for the production of BCJ2315 nitrilase from *E. coli* employed dithiothreitol (DTT) reducing agent during purification and eventual storage of the isolated enzyme[6] despite the fact that the final large scale biotransformations employed wet cells.[7] The use of reducing agents such as DTT is proposed to protect the catalytic cysteine residue from oxidative disulfide bond formation which would render the enzyme inactive. Indeed the requirement for reducing reagents has also been observed with other purified nitrilases, although high concentrations of DTT have been found to be detrimental to certain nitrilases.[8,9] DTT should also prevent the formation of additional intra- or intermolecular disulfide bonds which could inactivate the enzyme. Nitrilases have been shown to have structures made up from homodimers, and this quaternary structure, which could be destabilized through disulfide bond formation, is also responsible for higher observed activity.[10] In wet whole cells

however, the nitrilase enzyme is protected by the intracellular cytoplasmic reducing environment. This preparation has limitations in terms of handling, stability, and storage,[11] and therefore a dried enzyme formulation is often preferable.

In our initial screening studies, the lyophilized cell-free extract without additional additives showed some activity but was significantly lower compared to that achieved with the same equivalent charge of whole cell biomass, presumably due to oxidative degradation or deactivation due to thermal exposure during sonication. Chemical methods of cell lysis which do not generate heat such as BugBuster were not investigated due to the cost of their use on scale being prohibitive. In an effort to reduce any potential effect of oxidative degradation, a pretreatment of the CFE with DTT was evaluated. While our initial studies showed improved reactivity, achieving 50% conversion of cyanohydrin **2** in 3.5 h (10 g/L of **2**, phosphate buffer pH 7.4, 30 °C with 10% v/v DMSO), the effect was found to be variable in subsequent replicate studies. Due to this lack of robustness, we decided to focus instead on both wet and lyophilized whole cell preparations, the latter of which was more appealing due to its ease of handling, storage, and reproducibility. In addition, we investigated water immiscible solvents which would make a subsequent workup more straightforward and we switched to a higher pH buffer to minimize the potential to form HCN under the reaction conditions. After 3.5 h of reaction (67 g/L of **2**, Tris-HCl buffer pH 8.5, 30 °C with 10% v/v ethyl acetate), the product content as determined by HPLC area in the reaction mixture was 28% and 42% for wet and freeze-dried cells respectively, using 5% enzyme loading. In these studies, wet cell loadings were adjusted to ensure equal enzyme charge based on their dry weight relative to **2**. Based upon these results, the use of lyophilized whole cells was selected for further process optimization experiments via parallel assessment of single reaction parameters and process productivity.

Initial single parameter optimization efforts (reaction medium, temperature, pH, and solvent tolerance) using lyophilized whole cells were conducted at low substrate concentrations (5−10 g/L of **2**) so as to avoid any interfering inhibition effects and to omit the potential need for pH adjustment during the course of the reaction due to the formation of the carboxylic acid product. In addition, low

enzyme loadings were used to prevent the reaction from achieving 100% conversion, thereby enabling the impact of each process parameter to be assessed.

Reassessment of organic solvents on the activity of BCJ2315 nitrilase from lyophilized whole cells was performed using both water miscible and immiscible solvents (Table 1). Cosolvent volumes were kept at 10% v/v in order to maintain the solubility of the substrate within the reaction mixture. As observed in earlier optimization efforts for CFE BCJ2315, alcohols (entries 1−3) were once again found to be deleterious to the reaction, shutting down all activity while nonprotic solvents (entries 4−7) gave much better results. Although a good result was observed with DMSO, a water immiscible cosolvent was preferred for ease of workup and EtOAc provided the best combined outcomes for conversion and optical purity, with toluene not far behind.

A series of reactions were next performed to assess the influence of pH and temperature on the reaction outcome using 10% by weight lyophilized whole cell BCJ2315 nitrilase for the preferred cosolvents ethyl acetate and toluene (Table 2). The results reveal that higher pH had a positive effect on

Table 2. Influence of pH, Temperature, and Reaction Cosolvent on BCJ2315 Lyophilized Whole Cell Activity[a]

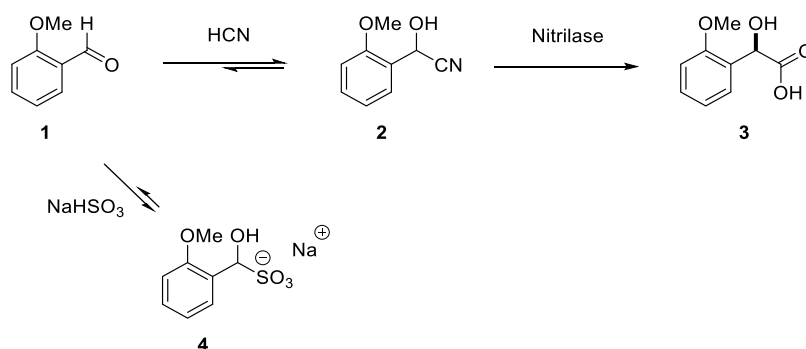| Entry	Solvent (10% v/v)	Temp (°C)	pH	Conversion after 8 h[b] (%)	% ee
1	Ethyl acetate	30	8.5[c]	97	90
2	Ethyl acetate	40	8.5[c]	83	90
3	Toluene	30	8.5[c]	97	86
4	Toluene	40	8.5[c]	97	86
5	Ethyl acetate	30	10.1[d]	97	93
6	Ethyl acetate	40	10.1[d]	77[e]	93
7	Toluene	30	10.1[d]	96	89
8	Toluene	40	10.1[d]	95	89
9	Ethyl acetate	30	10.7[d]	97	94
10	Ethyl acetate	40	10.7[d]	55[e]	94
11	Toluene	30	10.7[d]	95	90
12	Toluene	40	10.7[d]	95	90

[a]2 was solubilized in either 0.5 mL of ethyl acetate or toluene and added to BCJ2315 (20 mg of freeze-dried cells) in 4.5 mL of an appropriate pH buffer to a final concentration of 40 g/L of 2. Reaction mixtures were shaken at the indicated temperature for 8 h. [b]Determined by HPLC at 283 nm. Conversion was determined by [% AN 3 + % AN ent-3]/[% AN 1 + % AN 2 + % AN 3 + % AN ent-3]. [c]100 mM Tris-HCl buffer. [d]100 mM Bicarbonate-carbonate buffer. [e]Conversion reported here is % AN 3 + % AN ent-3 due to formation of significant impurity formation.

optical purity of the product. Raising the temperature from 30 to 40 °C did not have any detectable impact on product ee but did lead to increased enzyme deactivation in ethyl acetate as a cosolvent, and in turn incomplete reaction. This effect was observed across all ethyl acetate containing reactions, with poor conversion being obtained, even after 16 h.

Until now, process optimization had been developed using the preformed 2. However, a more cost-effective approach would be a one-pot process using readily available 2-methoxybenzaldehyde (1) as starting material. Given the promising results obtained thus far, it was decided to explore this one-pot reaction under biphasic conditions starting with the aldehyde and NaCN. Previous reports of similar one-pot processes had been limited due to enzyme deactivation by the benzaldehyde starting material which had led to the development of more complex fed-batch processes.[7b,12] Enzyme deactivation using BCJ2315 lyophilized whole cells had been observed early on in our reaction optimization efforts. While typical reaction conditions are expected to favor cyanohydrin formation over the aldehyde, this reaction is in equilibrium and thus some amount of enzyme deactivating aldehyde would always be present. This issue was expected to impact process robustness and cost due to the subsequent need for higher enzyme loadings to overcome enzyme deactivation and achieve full conversion. In addition, higher enzyme loadings would also complicate downstream product extraction and isolation operations. To avoid these potential issues, we hypothesized that sodium bisulfite in the reaction would sequester any free aldehyde as the corresponding bisulfite adduct, thereby reducing its ability to deactivate the enzyme. In this proposed process, the aldehyde would first react with bisulfite to form 4. Any remaining aldehyde may alternatively undergo cyanohydrin formation directly with HCN (Scheme 2) thereby working with the sodium bisulfite to lower the effective concentration of the inhibiting benzaldehyde.

Initial proof of principle studies for this one-pot process were successfully carried out on gram scale using 5% by weight lyophilized whole cell BCJ2315 in 9:1 water/ethyl acetate (0.49 M final substrate concentration). The reaction was performed using 1.1 equiv of NaHSO₃ and 1 equiv of NaCN, affording 3 in 93% ee and in 90% isolated yield after 48 h at 22 °C. Repeat studies were subsequently performed to evaluate the impact of temperature for this one-pot process under more challenging reaction conditions employing a lower 2.5 wt % lyophilized whole cell BCJ2315 loading. Reaction mixtures were prepared by mixing 1 volume of ethyl acetate with 7.5 volumes of an aqueous aldehyde−bisulfite adduct solution (prepared via dissolution of 1 in 0.979 M aqueous NaHSO₃).

Scheme 2. Proposed One-Pot DKR Route to (R)-2-Methoxymandelic Acid (3) via Bisulfite Adduct Formation

To this was added 1.5 volumes of 4.9 M aqueous NaCN solution dropwise (total reaction volume concentration = 100 g/L of **1**). These studies evaluated the reaction rate at 21, 30, and 37 °C by HPLC analysis at 1, 2.5, 4.5, 7, and 24 h.[13] This study revealed that while both reactions at 21 °C and at 30 °C showed complete consumption of the starting materials over 24 h, the reaction at 37 °C did not reach completion, presumably due to enzyme deactivation from both the high temperature and substrate concentration. Interestingly, lower reaction concentrations of 68 g/L of **1** (0.5 M) at this higher 37 °C temperature were tolerated and allowed the reaction to be complete, further highlighting this subtle interplay between substrate concentration and temperature for this process. Based on this observation, this effect was further investigated using more challenging lower whole cell enzyme loadings (2% by weight) to identify the preferred reaction conditions that enabled robust performance while maximizing throughput (Table 3). These results showed incomplete reactions for the

Table 3. Effect of Aldehyde and Temperature on Reaction Profile using Lyophilized Whole Cell BCJ2315[a]

Entry	Aldehyde Loading (g/L)	Temp (°C)	% AN **3** + % AN **ent-3** after 24 h[b] (%)	% ee
1	68	45	64	94
2	68	37	95	93
3	100	37	84	94
4	100	30	95	94
5	100	21	96	94
6	150	30	17	93
7	150	21	48−89	93
8	200	19−24	—[c]	N/A

[a]The reaction mixtures were prepared by mixing 7.5 volumesof aqueous aldehyde-bisulfite adduct solution, prepared via reaction of appropriate amount of **1** with 1.1 equiv of NaHSO$_3$ in water, with 1 volume of ethyl acetate, followed by dropwise addition of 1 equiv of NaCN in 1.5 volumes of water. BCJ2315 (2% by weight relative to **1**) was added, and the reaction mixture was stirred at the appropriate temperature. [b]Determined by HPLC. Full conversion was deemed achieved when no **2** was detected at 283 nm. Conversion was determined by [% AN **3** + % AN **ent-3**]/[% AN **1** + % AN **2** + % AN **3** + % AN **ent-3**].[15] [c]No **3** or **ent-3** was detected.

process using ethyl acetate cosolvent at higher reaction temperature and/or substrate concentrations. A further complicating factor was that at ambient temperatures and 100 g/L of **1** loading, the aqueous solution of the bisulfite-aldehyde adduct **4** used to prepare cyanohydrin **2** has a concentration of 0.979 M, which is near its saturation point of 1.02 M.[14] This was believed to be a contributing reason for the observed inconsistent results when increasing the aldehyde **1** loading to 150 g/L (Table 3, entry 7). For this reason, the target temperature and substrate concentration chosen were 21 °C and 100 g/L of **1** for the process, as it was expected to give the most consistent results regarding reaction rate, total turnover, and selectivity. As shown in Table 3, the ee of the product was not affected by changes to either substrate loading or temperature under these reaction conditions.

With suitable reaction conditions in hand, we began enzyme engineering nitrilase BCJ2315[6] to fit the process with the goal of improving substrate loading, enzyme robustness, and the enantioselectivity of **3**. A rational *in silico* approach was used to identify key enzyme residues for modification based on our previous success in efficiently re-engineering a transaminase

enzyme.[16] This approach was preferred since it often can explain the *in vitro* results while enabling exploration of the enzyme's multidimensional fitness landscapes, thereby allowing evolutionary studies to focus on smaller data sets of mutants at a fraction of the cost versus typical directed evolution approaches.

We began our rational engineering of BCJ2315 by constructing a homology model of the enzyme and submitting it for extensive molecular dynamics (MD) simulations to better sample the positions of all atoms in explicit solvent (Figure 1). These studies found the active center is predominately comprised of the anticipated catalytic triad (E48, K130 and C164), with the following residues that comprise the binding pocket: Y54, L56, W59, T134, E137, W165, W188, P189, S190, F191, S192, A197, A198, G202, P203, N206, L246, Q247, A248, G249, and G250.

The nitrilase reaction mechanism can be divided into three steps:[17] (1) The thiol group of the catalytic C164 which undergoes nucleophilic attack on the electrophilic carbon of the substrate nitrile group, forming a thioimidate intermediate; (2) the thioimidate intermediate is hydrolyzed forming a second acyl enzyme intermediate, with release of ammonia; (3) and finally the acyl enzyme intermediate is hydrolyzed to produce the carboxylic acid. In this overall process, the first step of the reaction mechanism should be rate limiting and was therefore chosen as the initial enzyme state for docking of the (*R*)- and (*S*)-substrates.

Homology model validation was conducted by docking (*R*)-2-chloromandelonitrile and (*S*)-2-chloromandelonitrile to WT BCJ2315 and comparing computation findings with previously reported experimental findings.[7] This analysis found the binding of (*R*)-2-chloromandelonitrile was better than that of its enantiomer, as the coordination between the substrate nitrile carbon and the C164 thiol group is shorter for (*R*)-2-chloromandelonitrile.[13] Docking of our substrates ((*R*)-**2** and (*S*)-**2**) in this validated enzyme model revealed that the reaction coordinate for the first step is shorter and the angle of the nucleophilic attack is better for (*R*)-**2** and therefore potentially closer to the Michaelis−Menten complex (Figure 2). Moreover, (*R*)-**2** is able to stabilize stronger intermolecular interactions within the active site via hydrogen bonding of the S192 side chain with the oxygen of the methoxy group and also by hydrogen bonding of W165 with the hydroxyl group of (*R*)-**2**. Both interactions are not present in the docking pose of the (*S*)-**2**. These findings again correlate to the experimentally observed selective formation of **3** from (*R*)-**2** by BCJ2315.

In silico model analysis focused predominately on identifying favorable mutations of two general types: first, active site mutations that could improve selectivity by (1) increasing the binding affinity for the (*R*)-**2** and (2) decrease the step 1 reaction coordinate of the (*R*)-**2** while subsequently increasing it for the (*S*)-**2**, and second, through B-factor analysis using four replicate 50 ns MD simulations of BCJ2315 to identify flexible residues/regions of the enzyme that could be modified to improve structural stability.[13] Additional mutants were also selected from previous literature reports and through coevolution analysis of nitrilase sequences.[7a] In total, 96 mutants were assessed experimentally in the first round of *in vitro* screening which revealed that a substantial number of mutants were able to improve selectivity and/or activity/stability.[13] A list of mutants which gave either increased selectivity and conversion or an increase in both, relative to WT, are detailed in Table 4. All mutants were expressed at the
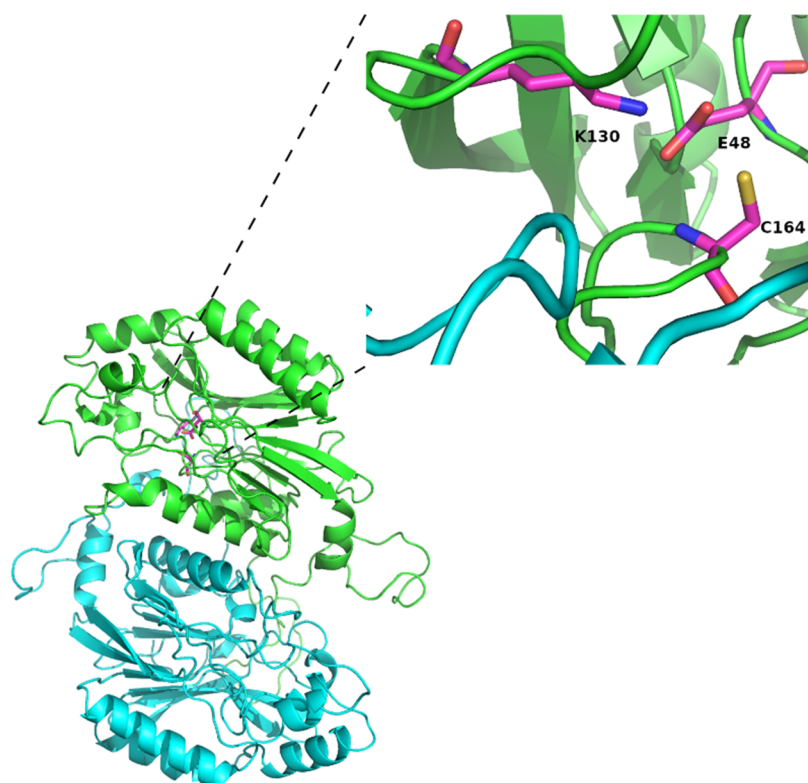
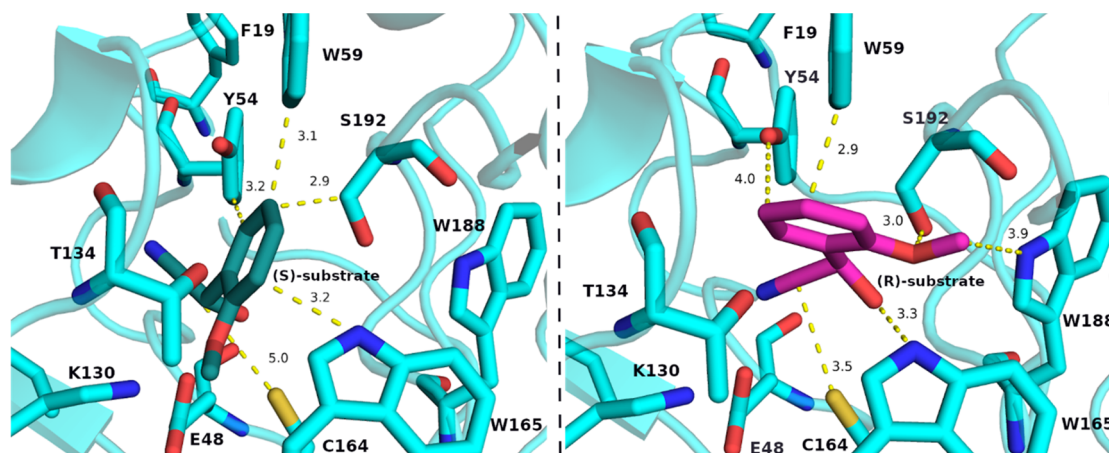**Figure 1.** MD Reference structure of nitrilase BCJ2315.

Figure 2. NIT BCJ2315 docking for (S)-**2** (left) and (R)-**2** (right). Distances are shown in Å.

same time under the same conditions in 96 well plate format. SDS-PAGE analysis was performed on the soluble cell lysate (freeze−thaw lysis) to ascertain if major variations in enzyme expression were responsible for the increased conversion performance noted in the best performing mutants.[13] This analysis showed that the mutants which resulted in higher activity during screening did not have a significantly higher level of soluble NIT expression compared to the WT. Based on these initial results the best performing mutants from small scale testing (M24-S192P, M25-S192G, M43-Y199Q, and M65-M232V) were grown at 1 L fermentation scale for subsequent gram scale evaluation.

Gram scale time course studies of the best performing mutant nitrilases from Table 4 versus WT BCJ2315 were conducted with 5% by weight enzyme loading relative to **1** (total concentration 100 g/L of **1**) using the optimized one-pot

procedure detailed above in order to assess their robustness (Figure 3). These reactions were run for longer than the initial screen (Table 4) with samples taken at multiple time points and analyzed by HPLC to determine conversion. Variants M65-M232V and M43-Y199Q were found to have very similar activity to WT, with the remaining mutants less active. Confirming the screening results, variants M24-S192P and M25-S192G showed excellent selectivity (98% and 97% ee, respectively); however, M24-S192P showed rapid enzyme deactivation resulting in poor conversion. Similarly, M25-S192G failed to fully convert the substrate, though its deactivation was much slower compared to M24-S192P. Mutants M65-M232V and M43-Y199Q did not show selectivity improvement versus the WT but did reach full conversion of **2**.

E

Table 4. Best Performing First Generation Mutants of BCJ2315[a]

Mutant ID	Enzyme Mutation	% ee[b]	Conversion (%)[b]
WT	WT	93.3	25.5
M77	A323S	90.8	33.9
M55	A108N	91.4	38.9
M65	M232V	91.9	44.0
M49	A64E	92.8	33.3
M10	W59F	93.5	37.2
M93	L201I	93.9	31.6
M42	Y199C	94.2	36.9
M43	Y199Q	93.7	37.3
M4	T49L	94.3	37.5
M25	S192G	97.0	27.6
M24	S192P	97.7	26.5

[a]0.5 mg of freeze-dried whole cells enzymes were incubated in a 96-well plate with 10 mg of **2** at a concentration of 10 mg/mL in a 10:1 mixture of 0.1 M sodium carbonate buffer (pH 9) and EtOAc at room temperature in a microplates shaker at 1500 rpm for 2 h. [b]Determined by HPLC at 283 nm. Conversion was determined by [%AN **3** + % AN **ent-3**]/[% AN **1** + % AN **2** + % AN **3** + % AN **ent-3**].
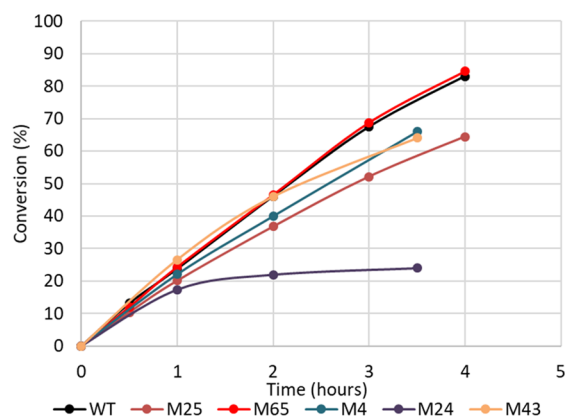

Figure 3. Time course study for select best performing first generation mutants. Determined by HPLC at 283 nm. Conversion was determined by [%AN **3** + % AN **ent-3**]/[% AN **1** + % AN **2** + % AN **3** + % AN **ent-3**]

Although the first generation of mutants failed to identify a mutant NIT that addressed both selectivity and activity, a second generation series of double mutants combining the increased selectivity of M25-S192G with the improved activity of M43-Y199Q and M65-M232V was deemed worthwhile for further evaluation. Evaluation of these double mutant combinations on gram scale using the one-pot conditions (5% by weight lyophilized whole cell, 22 °C) revealed that the double mutant M100-S192G-M232V gave the best performance, achieving improved stability compared to the single mutation variant M25-S192G while maintaining the selectivity of the M65-M232V variant (97.0% ee and 72% conversion vs 97.0% ee and 64% conversion for M25-S192G over 4 h, Figure 4), and with only slightly lower activity than the wild type enzyme. Additionally, we note that analysis of the crude reaction mixture did not show any presence of the corresponding mandelic amide, a typical impurity observed in nitrilase processes, simplifying our downstream isolation processes.

The observed selectivity improvement of M100-S192G-M232V versus WT BCJ2315 can be rationalized through the
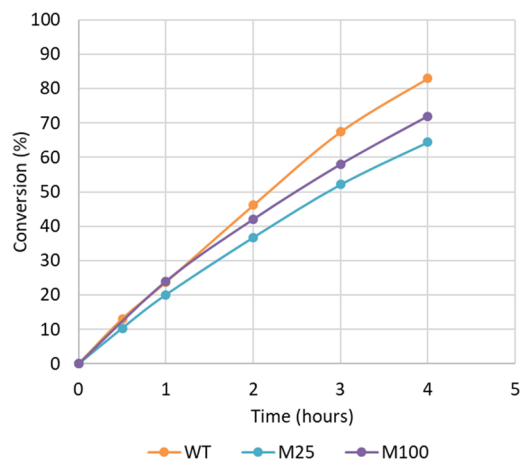

Figure 4. Time course study for M100, M25, and WT BCJ2315 enzymes. Determined by HPLC at 283 nm. Conversion was determined by [%AN **3** + % AN **ent-3**]/[% AN **1** + % AN **2** + % AN **3** + % AN **ent-3**].

substantial change on the substrate active site posed imparted via the S192G mutation. In mutant S192G, the T134 side chain forms a stabilizing hydrogen bond with the (R)-**2** methoxy group, while in the WT the substrate methoxy group instead forms a stabilizing hydrogen bond with the S192 side chain. As a result, for the first reaction step (nucleophilic attack of the SH group of the active center Cys on the electrophilic carbon of the substrate nitrile group), the reaction coordinate of (R)-**2** is shorter (2.9 Å) and the angle of the attack is better than in the WT ((R)-**2** (3.5 Å) (Figure 2 and Figure 5). Selective conversion of the (R)-substrate should therefore occur at a higher rate for the S192G mutant than the WT BCJ2315.

Based on B-factors analysis, M232 is predicted to be an unstable residue.[13] Mutation M232V removes the methionine residue from the surface, potentially preventing associated oxidation issues and therefore increasing the intermolecular interactions within a hydrophobic pocket which contribute to the increased structural stability of the enzyme (Figure 6). The combination of both mutations (S192G and M232V) was required to overcome the reduced stability observed with the selectivity enhancing S192G mutation alone.

With a robust and highly selective reaction process in hand, we began optimization of the downstream process. At the end of the hydrolysis we noted that the reaction was a suspension of cells at pH ≈ 8.4. We envisioned the initial process workup operations to involve a Celite filtration to remove cellular debris followed by adding an additional 1 volume of ethyl acetate to generate a layer cut and remove unreacted benzaldehyde from the aqueous workup stream containing **3**. Additional stress studies were also carried out to investigate the downstream impact of removing the ethyl acetate addition and layer cut altogether. It was found that without this unit operation any remaining benzaldehyde could still be completely purged to the current in-process control limit of <3% **1**, in the final ethyl acetate/diisopropyl ether/heptanes crystallization of **3**. Ultimately, the minimal yield losses (<0.25% **3**) along with downstream process impurity concerns led us to retain this layer cut operation. While our initial Celite filtrations were slow, they were successful in removing the bulk of the cellular debris, enabling visualization of the resulting cloudy white water and clear ethyl acetate layers after an
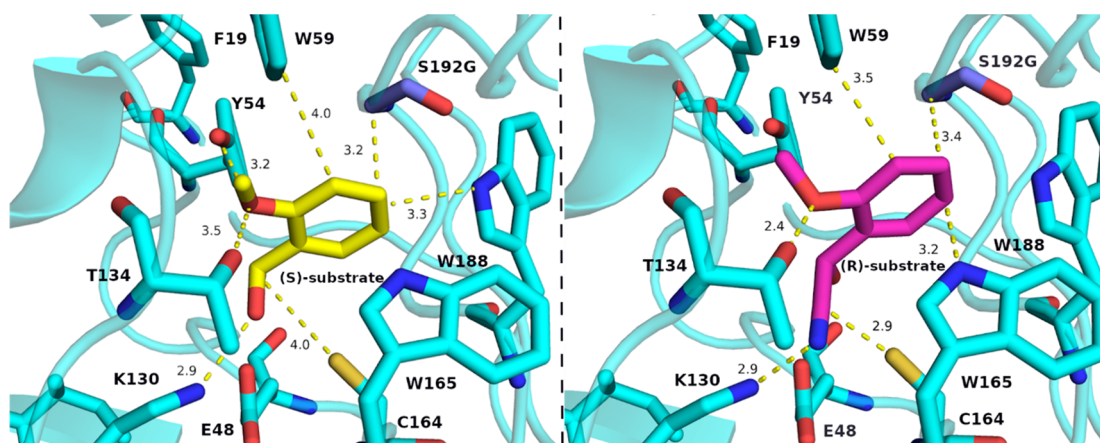
Figure 5. NIT BCJ2315_S192G docked to (*S*)-**2** (left) and (*R*)-**2** (right). Distances shown are in Å.
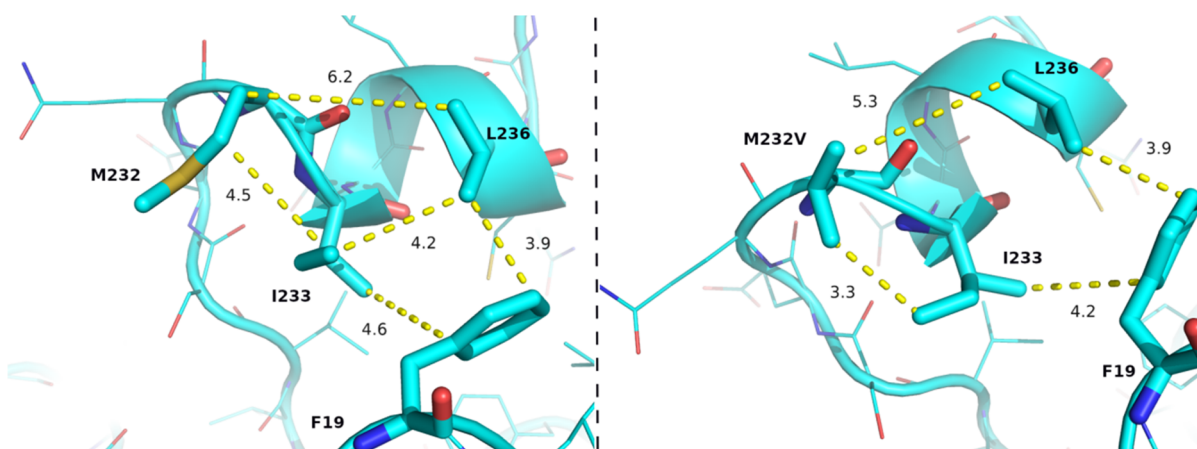

Figure 6. BCJ2315 (left) vs BCJ2315_M232V (right). Distances shown are in Å.

additional 1 volume of both ethyl acetate and water were added. Further improvement in both the filtration time and initial layer cut at pH ≈ 8 was also possible through the use of an Akta Flux S cross-flow filtration system using a hollow fiber cartridge containing a 0.2 μm polysulfone membrane.

In the next step of the isolation process the acidification to pH ≈ 1 with conc. HCl and extraction of **3** using ethyl acetate presented a significant operational challenge due to the formation of a white emulsion in the ethyl acetate layer due to emulsification of solubilized protein carryover at this low pH. Spiking studies for different organic comixtures using ethyl acetate/M100 lyophilized cell supernatant revealed a significant increase in solubility of **3** versus unspiked ethyl acetate, leading to concerns about protein carryover and its impact on mother liquor losses in the crystallization. As such, efforts were focused on enzyme removal and a resolution to the emulsion challenge. Initial studies focused on protein removal either through precipitation by aging for 2 h at 60 and 90 °C prior to Celite filtration or through treatment at pH 10 overnight in an effort to digest or break down proteins. In all cases no significant improvement was observed after acidification to pH ≈ 1. Several salt additives were then evaluated in an effort to break the emulsion. While charging 1.5× NaCl, CaCl₂ or Na₂SO₄ after pH adjustment did not lead to any significant change in the emulsion formation, fortuitously, MgSO₄ was found to break the emulsion forming a thin rag layer at the interface that could be subsequently polish filtered to reveal a

very clear layer cut. Additional optimization found that increasing the MgSO₄ loading from 1.5× to 2× more effectively resulted in collapse of the problematic protein emulsion (Figure 7).

Following layer cut of the resulting clear ethyl acetate/water layers, the pH ≈ 1 aqueous layer was further back extracted

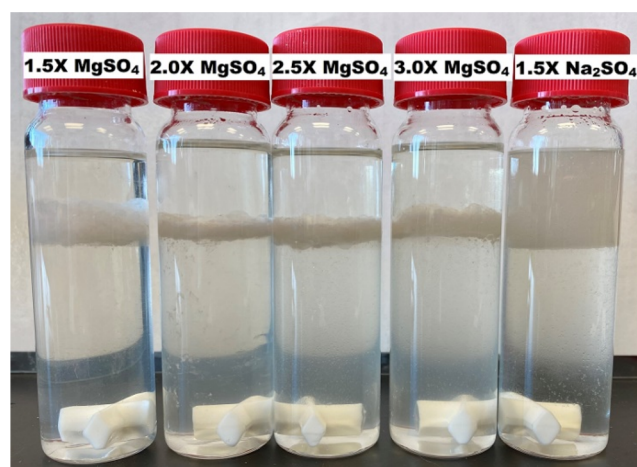**Figure 7.** Impact of select salt additives and their loading on emulsion formation at pH ≈ 1.

with ethyl acetate twice in order to minimize loss of **3** to the aqueous layer (<0.25% **3**).

Our initial crystallization efforts for **3** focused on a streamlined process whereby the organic layers were combined and concentrated to 1.5 volumes under vacuum and heated to 50 °C to ensure full dissolution followed by ramp cooling to 25−30 °C, seeding, and further cooling to 0 °C prior to filtration. While this process gave a mobile slurry and ee upgrade to >99.0%, mother liquor losses were unacceptably high (15−25%), owing to the high solubility of **3** in ethyl acetate (ca. 6 mL ethyl acetate/g **3**). Solubility screening of **3** in a wide range of solvents identified a small handful of potential antisolvents for the crystallization of **3**: heptane(s), toluene, xylenes, and ethereal solvents such as dibutyl ether and diisopropyl ether. After extensive screening of various solvent combinations, the preferred crystallization process distilled the combined ethyl acetate layers to 1.5 volumes under vacuum followed by addition of 1.5× diisopropyl ether antisolvent. The mixture was then heated to 65 °C for 1 h to ensure full dissolution and then cooled to 50 °C and held at 50 °C for 3 h. During this holding process a hazy reaction mixture was observed, at which point seeding was performed to produce a mobile slurry. In order to minimize mother liquor losses, heptanes (1.0×) was then slowly added at 50 °C over ca. 2 h to prevent oiling out of **3**. Cooling and filtration at −20 °C afforded **3** in 60−75% yield and in high (96−100%) ee and good assay purity with acceptable mother liquor losses (ca. 10% yield).

Enzyme analysis using the Bradford assay for the finalized process waste streams and final solid was also evaluated to determine effective purge points and to assess downstream process risk. As shown in Table 5, several effective protein

Table 5. Enzyme Content in Waste Streams for Finalized Process for 3

Analysis Point	Protein Concentration[a] (ppm)	Weight % of Total Biomass Charged
Initial ethyl acetate layer waste stream after Celite filtration (pH ≈ 8)	553	1.7
Aqueous layer waste stream after final ethyl acetate extraction (pH ≈ 1)	Not detected[b]	0.0
Mother liquor waste stream (ethyl acetate/diisopropyl ether/heptanes)	391	2.0
Isolated **3**	91	0.2

[a]Determined using Bradford assay. See Supporting Information for details. [b]Detection limit = 10 ppm.

purge points were built into the process, the main ones being the initial ethyl acetate wash and final isolation. Together, these two points enable 95% purge of the protein carried over after the initial Celite filtration, which was deemed suitable for our intended downstream process use of **3**.

CONCLUSION

The concurrent process development and enzyme engineering activities resulted in the development of a superior process versus what could be achieved by performing these activities individually without considering their respective impacts on each other. This approach helped identify initial protein preparation limitations and enabled the concurrent adjustment of the process chemistry conditions to produce a more robust

nitrilase process. Rational protein engineering to improve enzyme selectivity and robustness using *in silico* analysis identified a number of favorable mutations via active site and B-factor analysis for initial evaluation. This efficient and low-cost approach led to the identification of two beneficial mutations over the WT nitrilase with respect to enantioselectivity and robustness. A plug-and-play enzyme change was feasible without problems; the improved variant enzyme gave similar activity and higher product enantioselectivity in conditions developed for maximized enzymatic turnover with the wild type. Reaction design identified enzyme deactivation by the aldehyde as a key obstacle for achieving a robust one-pot process. Ultimately, this observation led to the discovery that the addition of sodium bisulfite could prevent this deactivation thereby allowing for a simplified high substrate loading process that avoided a fed-batch approach. Downstream process optimization activities also identified magnesium sulfate as a critical workup additive to avoid emulsion formation, allowing for the isolation of the desired final product in good yield and in excellent enantioselectivity with high control of residual protein content.

EXPERIMENTAL SECTION

Solvents and reagents were obtained from commercial sources and used without further purification. ^1H NMR was performed on a Bruker Avance III HD 400 MHz spectrometer (^1H NMR at 400 MHz, ^{13}C NMR at 101 MHz) with solvent resonances as the internal standard (^1H NMR: DMSO-$d6$ at 2.50 ppm; ^{13}C NMR: DMSO-$d6$ at 39.52 ppm). ^1H NMR data are reported as follows: chemical shift, integration, multiplicity (s = singlet, d = doublet, t = triplet, dd = doublet of doublets, dt = doublet of triplets), and coupling constants (Hz). HPLC/UPLC was performed on an Agilent 1260 system equipped with a PDA detector. Bradford assay analysis was performed using an Agilent Cary 60 UV−vis spectrophotometer equipped with Cary Win UV software using BSA (lyophilized powder, Sigma) and Coomassie Plus Assay Reagent (ThermoFisher Scientific).

Preparation of (R)-2-Methoxymandelic Acid (3). To a solution of 2-methoxybenzaldehyde (40.00 g, 293.8 mmol, 1.00 equiv) in ethyl acetate (40.03 g) was added solid NaHSO$_3$ (30.58 g, 293.9 mmol, 1.00 equiv) and water (300.04 g). After the addition was complete, the reaction mixture was agitated for an additional ca. 60 min, resulting in a colorless hazy solution. To this reaction mixture was then slowly added a solution of NaCN (14.69 g, 299.7 mmol, 1.02 equiv) in water (60.03 g) while maintaining the pot temperature below 25 °C. After the addition was complete, the reaction mixture was agitated for an additional ca. 60 min. To this reaction mixture was then added M100 dried whole cell enzyme (2.04 g, 5% w/w relative to the aldehyde). After the addition was complete, the reaction mixture was agitated for an additional 24 to 48 h until the reaction was deemed complete by HPLC. The reaction mixture was then filtered through a layer of Celite, and the reactor and Celite were rinsed forward with water (40.02 g). The combined filtrate (caution: trace NaCN may still be present in the filtrate) were washed with ethyl acetate (40.03 g). The organic layer was discarded, and the aqueous layer was acidified to pH 1 with conc. HCl resulting in formation of an emulsion. MgSO$_4$ (80.05 g) was then added to the aqueous layer, and the resulting solution was stirred for ca. 15 min to break the emulsion. Ethyl acetate (100.04 g) was then added, and the resulting rag layer at the interface was removed via a

polish filtration. The organic layer was removed, and the aqueous layer was extracted with ethyl acetate (2 × 100.05 g). The combined organic layers were concentrated under vacuum to approximately 60 mL (ca. 1.5 volumes) using a reactor jacket temperature of approximately 55 °C. Diisopropyl ether (60.03 g) was then added in one portion to the resulting pale yellow hazy solution and agitated at about 65 °C for approximately 1 h. The reaction mixture was then cooled over 2 h to approximately 50 °C, and then seed (0.1216 g) was charged resulting in slurry formation. Once a slurry was confirmed, heptanes (40.05 g) was charged over not less than 2 h. After addition, the slurry was then cooled over about 7 h to approximately −20 °C and agitated at −20 °C for not less than 3 h. The final product was filtered and washed with precooled diisopropyl ether (40.05 g) at about −10 °C. The final solids were dried at 45 °C in a vacuum oven with nitrogen sweep for not less than 4 h to provide 37.27 g of the title compound (70% yield, 99.10% assay purity, 96.89 ee% determined by UPLC at 283 nm) as a white solid. Average yields ranged from 60% to 75% with a purity range of 95−103 assay% by qNMR and 96−100% ee by UPLC at 283 nm.

^{1}H NMR (DMSO-d_6, 400 MHz) δ: 12.34 (1H, broad s), 7.35 (1H, dd, J = 1.8, 7.4 Hz), 7.27 (1H, dt, J = 2.0, 7.8 Hz), 6.97 (1H, d, J = 8.4 Hz), 6.94 (1H, dt, J = 0.8, 3.6 Hz), 5.30 (1H, s), 3.77 (3H, s); ^{13}C NMR (DMSO-d_6, 100 MHz) δ: 174.4, 156.6, 129.1, 128.8, 128.0, 120.4, 111.2, 67.0, 55.6.

ASSOCIATED CONTENT

◆ Supporting Information

The Supporting Information is available free of charge at https://pubs.acs.org/doi/10.1021/acs.oprd.1c00250.

> Complete experimental procedures and characterization data including: biocatalyst preparation, computational methods of homology model building and MD simulation, nitrilase mutant preparation and evaluation (rounds 1 and 2), preparation of bisulfite adduct 4, Bradford assay method, HPLC method, NMR spectra (PDF)

AUTHOR INFORMATION

Corresponding Author

Luke D. Humphreys − *Gilead Alberta ULC, Edmonton, Alberta, Canada T6S 1A1;* ◉ orcid.org/0000-0001-6497-4339; Email: Luke.Humphreys@Gilead.com

Authors

Mark E. Scott − *Gilead Alberta ULC, Edmonton, Alberta, Canada T6S 1A1;* Present Address: Flare Therapeutics, 215 First Street, Suite 150, Cambridge, Massachusetts, 02142, United States

Xiaotian Wang − *Gilead Alberta ULC, Edmonton, Alberta, Canada T6S 1A1*

Michael J. Geier − *Gilead Alberta ULC, Edmonton, Alberta, Canada T6S 1A1*

Balamurali Kannan − *Gilead Alberta ULC, Edmonton, Alberta, Canada T6S 1A1*

Johann Chan − *Gilead Sciences, Inc, Foster City, California 94404, United States;* Present Address: Praxis Precision Medicines, One Broadway, Cambridge, Massachusetts, 02142, United States

Gareth Brown − *Almac Sciences, Craigavon BT63 5QD, U.K.*

Daniel F. A. R. Dourado − *Almac Sciences, Craigavon BT63 5QD, U.K.*

Darren Gray − *Almac Sciences, Craigavon BT63 5QD, U.K.*

Stefan Mix − *Almac Sciences, Craigavon BT63 5QD, U.K.*

Aliaksei Pukin − *Almac Sciences, Craigavon BT63 5QD, U.K.*

Complete contact information is available at:
https://pubs.acs.org/10.1021/acs.oprd.1c00250

■ ABBREVIATIONS

% AN	percent area normalization
CFE	cell free enzyme
EC	enzyme commission
HPLC	high performance liquid chromatography
MD	molecular dynamics
NIT	nitrilase
UPLC	ultra high performance liquid chromatography
WT	wild type
X	weight ratio

■ REFERENCES

(1) (a) Wu, S.; Snajdrova, R.; Moore, J. C.; Baldenius, K.; Bornscheuer, U. T. Biocatalysis: Enzymatic Synthesis for Industrial Applications. *Angew. Chem., Int. Ed.* **2021**, *60*, 88−119. (b) Abdelraheem, E. M. M.; Busch, H.; Hanefeld, U.; Tonin, F. Biocatalysis Explained: From Pharmaceutical to Bulk Chemical Production. *React. Chem. Eng.* **2019**, *4*, 1878−1894. (c) *Pharmaceutical Biocatalysis Chemoenzymatic Synthesis of Active Pharmaceutical Ingredients*; Grunwald, P., Ed.; Jenny Stanford Publishing: Singapore, 2020.

(2) (a) *Enzyme Nomenclature 1992: Recommendations of the Nomenclature Committee of the International Union of Biochemistry and Molecular Biology on the nomenclature and classification of enzymes*; Webb, E., Ed.; Academic Press: New York, 1992. (b) Enzyme Nomenclature. https://www.qmul.ac.uk/sbcs/iubmb/enzyme/ (accessed 2021-06-03).

(3) Shen, J.-D.; Cai, X.; Liu, Z.-Q.; Zheng, Y.-G. Nitrilase: A Promising Biocatalyst in Industrial Applications for Green Chemistry. *Crit. Rev. Biotechnol.* **2021**, *41*, 72−93.

(4) (a) Pace, H. C.; Brenner, C. The Nitrilase Superfamily: Classification, Structure and Function. *Genome Biol.* **2001**, *2*, reviews0001.1. (b) Brenner, C. Catalysis in the Nitrilase Superfamily. *Curr. Opin. Struct. Biol.* **2002**, *12*, 775−782.

(5) See for example: (a) Baum, S.; van Rantwijk, F.; Stolz, A. Application of a Recombinant Escherichia coli Whole-Cell Catalyst Expressing Hydroxynitrile Lyase and Nitrilase Activities in Ionic Liquids for the Production of (S)-Mandelic Acid and (S)-Mandeloamide. *Adv. Synth. Catal.* **2012**, *354*, 113−122. (b) Bhatia, S. K.; Mehta, P. K.; Bhatia, R. K.; Bhalla, T. C. Optimization of Arylacetonitrilase Production from Alcaligenes sp. MTCC 10675 and its Application in Mandelic Acid Synthesis. *Appl. Microbiol. Biotechnol.* **2014**, *98*, 83−94. (c) He, Y.-C.; Zhang, Z.-J.; Xu, J.-H.; Liu, Y.-Y. Biocatalytic Synthesis of (R)-(2)-Mandelic Acid from Racemic Mandelonitrile by Cetyltrimethylammonium Bromidepermeabilized Cells of Alcaligenes Faecalis ECU0401. *J. Ind. Microbiol. Biotechnol.* **2010**, *37*, 741−750. (d) Ni, K.; Wang, H.; Zhao, L.; Zhang, M.; Zhang, S.; Ren, Y.; Wei, D. Efficient Production of (R)-(−)-Mandelic Acid in Biphasic System by Immobilized Recombinant E. coli. *J. Biotechnol.* **2013**, *167*, 433−440. (e) Petříčková, A.; Sosedov, O.; Baum, S.; Stolz, A.; Martínková, L. Influence of Point Mutations Near

the Active Site on the Catalytic Properties of Fungal Arylacetonitrilases from *Aspergillus niger* and *Neurospora crassa*. *J. Mol. Catal. B: Enzym.* **2012**, *77*, 74−80. (f) Sosedov, O.; Stolz, A. Random Mutagenesis of the Arylacetonitrilase from *Pseudomonas fluorescens* EBC191 and Identification of Variants, Which Form Increased Amounts of Mandeloamide from Mandelonitrile. *Appl. Microbiol. Biotechnol.* **2014**, *98*, 1595−1607. (g) Wang, S.-Z.; Wang, Z.-K.; Gong, J.-S.; Qin, J.; Dong, T.-T.; Xu, Z.-H.; Shi, J.-S. Improving the Biocatalytic Performance of Co-immobilized Cells Harboring Nitrilase via Addition of Silica and Calcium Carbonate. *Bioprocess Biosyst. Eng.* **2020**, *43*, 2201−2207. (h) Zhang, X.-H.; Liu, Z.-Q.; Xue, Y.-P.; Wang, Y.-S.; Yang, B.; Zheng, Y.-G. Production of *R*-Mandelic Acid Using Nitrilase from Recombinant *E. coli* Cells Immobilized with Tris(Hydroxymethyl)Phosphine. *Appl. Biochem. Biotechnol.* **2018**, *184*, 1024−1035. (i) Zhang, X.-H.; Wang, C.-Y.; Cai, X.; Xue, Y.-P.; Liu, Z.-Q.; Zheng, Y.-G. Upscale Production of (*R*)-Mandelic Acid with a Stereospecific Nitrilase in an Aqueous System. *Bioprocess Biosyst. Eng.* **2020**, *43*, 1299−1307.

(6) Wang, H.; Sun, H.; Wei, D. Discovery and Characterization of a Highly Efficient Enantioselective Mandelonitrile Hydrolase from *Burkholderia Cenocepacia* J2315 by Phylogeny-Based Enzymatic Substrate Specificity Prediction. *BMC Biotechnol.* **2013**, *13*, 14.

(7) (a) Wang, H.; Gao, W.; Sun, H.; Chen, L.; Zhang, L.; Wang, X.; Wei, D. Protein Engineering of a Nitrilase from *Burkholderia Cenocepacia* J2315 for Efficient and Enantioselective Production of (*R*)-2-Chloromandelic acid. *Appl. Environ. Microbiol.* **2015**, *81*, 8469−8477. (b) Wang, H.; Sun, H.; Gao, W.; Wei, D. Efficient Production of (*R*)-o-Chloromandelic Acid by Recombinant *Escherichia coli* Cells Harboring Nitrilase from *Burkholderiacenocepacia* J2315. *Org. Process Res. Dev.* **2014**, *18*, 767−773.

(8) Kobayashi, M.; Nagasawa, T.; Yamada, H. Nitrilase of *Rhodococcus Rhodochrous* J1. Purification and Characterization. *Eur. J. Biochem.* **1989**, *182*, 349−356.

(9) (a) Dennett, G. V.; Blamey, J. M. A New Thermophilic Nitrilase from an Antarctic Hyperthermophilic Microorganism. *Front. Bioeng. Biotechnol.* **2016**, *4*, 5. (b) Khandelwal, A. K.; Nigam, V. K.; Vidyarthi, A. S.; Ghosh, P. Evaluation of Various Ions and Compounds on Nitrilase Produced from *Streptomyces* sp. *Artif. Cells, Blood Subst. Immobil. Biotechnol.* **2010**, *38*, 13−18.

(10) Thuku, R. N.; Brady, D.; Benedik, M. J.; Sewell, B. T. Microbial Nitrilases: Versatile, Spril Forming, Industrial Enzymes. *J. Appl. Microbiol.* **2009**, *106*, 703−727.

(11) (a) Kiziak, C.; Conradt, D.; Stolz, A.; Mattes, R.; Klein, J. Nitrilase from *Pseudomonas fluorescens* EBC191: Cloning and Heterologous Expression of the Gene and Biochemical Characterization of the Recombinant Enzyme. *Microbiology* **2005**, *151*, 3639−3648. (b) Banerjee, A.; Kaul, P.; Banerjee, U. C. Enhancing the Catalytic Potential of Nitrilase from *Pseudomonas putida* for Stereoselective Nitrile Hydrolysis. *Appl. Microbiol. Biotechnol.* **2006**, *72*, 77−87. (c) Banerjee, A.; Kaul, P.; Banerjee, U. C. Erratum to: Enhancing the Catalytic Potential of Nitrilase from Pseudomonas putida for Stereoselective Nitrile Hydrolysis. *Appl. Microbiol. Biotechnol.* **2017**, *101*, 6299. (d) Howden, A. J.; Preston, G. M. Nitrilase Enzymes and their role in Plant-microbe Interactions. *Microb. Biotechnol.* **2009**, *2*, 441−451.

(12) Wang, H.; Fan, H.; Sun, H.; Zhao, Li; Wei, D. Process Development for the Production of (*R*)-(−)-Mandelic Acid by Recombinant *Escherichia coli* Cells Harboring Nitrilase from *Burkholderia cenocepacia* J2315. *Org. Process Res. Dev.* **2015**, *19*, 2012−2016.

(13) See Supporting Information for more details.

(14) Determined by preparing **4** and measuring the amount of water needed to fully dissolve a known amount of compound with shaking. See Supporting Information for more details.

(15) Conversion calculations did not include the % AN of the bisulfite adduct **4** as it was found to be unstable under the sample preparation/method analysis, converting to the aldehyde which was measured instead.

(16) Dourado, D. F. A. R.; Pohle, S.; Carvalho, A. T. P.; Dheeman, D. S.; Caswell, J. M.; Skvortsov, T.; Miskelly, I.; Brown, R. T.; Quinn, D. J.; Allen, C. C. R.; Kulakov, L.; Huang, M.; Moody, T. S. Rational Design of a (*S*)-Selective-Transaminase for Asymmetric Synthesis of (1*S*)-1-(1,1′-biphenyl-2-yl)ethanamine. *ACS Catal.* **2016**, *6*, 7749−7759.

(17) Kobayashi, M.; Goda, M.; Shimizu, S. Nitrilase Catalyzes Amide Hydrolysis as well as Nitrile Hydrolysis. *Biochem. Biophys. Res. Commun.* **1998**, *253*, 662−666.